Effect of Interfacial Permeability on Droplet Relaxation in Biopolymer-Based Water-in-Water Emulsions

Elke Scholten, Joris Sprakel, Leonard M. C. Sagis, and Erik van der Linden*

Food Physics Group, Department of Agrotechnology and Food Sciences, Wageningen University, Bomenweg 2, 6703 HD Wageningen, The Netherlands

Received September 27, 2005; Revised Manuscript Received November 9, 2005

In this paper, we show that for aqueous phase-separated biopolymer mixtures (water-in-water emulsions) both interfacial tension and permeability of the interface are important for the relaxation process of deformed droplets. We give an expression for the characteristic relaxation time that contains both contributions. With this description, the interfacial tension and the permeability can be deduced from cessation-of-flow experiments. The results show that for samples that are very close to the critical point the interfacial tension, calculated without taking into account the permeability, are overestimated significantly. For samples close to the critical point, the permeability has to be taken into account in the description for the relaxation time to get a reliable estimation of the interfacial tension. Our experiments show that for these systems the effective permeability is inversely proportional to the interfacial tension, $\lambda_{\text{eff}} \propto 1/\gamma$, and proportional to the square of the interfacial thickness, $\lambda_{\text{eff}} \propto \xi^2$. We find that the permeability is related to an effective diffusion coefficient as $D_{\text{eff}} \propto \lambda\gamma_{\text{eff}}$. From this relation, we find that the diffusion coefficient is equal to $0.9 \cdot 10^{-9}$ m^2/s, which is close to the self-diffusion coefficient of water; $D_{\text{w}}^0 = 2.3 \cdot 10^{-9}$ m^2/s. This indicates that only water diffuses through the interface, and the diffusion coefficient is independent of the composition of the system for the concentration regime that is used.

Introduction

Phase separation is a common phenomenon that often occurs in polymer or biopolymer mixtures. Phase separation results in the formation of an interface, separating two bulk phases, and the interfacial properties are interesting from both a fundamental and an applied point of view. Many industries (food, pharmaceutical, plastics, personal care) make use of this phenomenon to create a diversity of products, and the properties of these products, such as stability, shelf life, and sensorial perception, are strongly influenced by the morphologies (droplets dispersed in a matrix, bicontinuous phases) formed after phase separation has occurred. In the plastic industry, mixtures of immiscible synthetic polymers are used to create a large variety of soft and hard composites. In the food industry, phase separation is used in the production of low-calorie products as a substitute for fatty products. To obtain the right sensory perception, such as mouth-feel, the morphology of the structures is a critical parameter. During the fabrication process, these products are exposed to flow fields, which influence their morphology (deformation, breakup, coalescence). The interplay between viscous forces and interfacial forces (such as interfacial tension) determines the magnitude of the changes in the morphology. Understanding the phase separation process and the resulting interfacial properties are key ingredients to influence and control product properties.

In the past decade, extensive research has been performed on polymer blends[1−9] and biopolymer mixtures.[10−16] In most of these investigations, dispersions of droplets of one phase in a matrix of the other phase are subjected to different types of flow, and the effects on the morphology are investigated with methods such as the deformed drop retraction[1,2,6] or droplet deformation method.[5,7,10−13,15,16] The deformation of droplets in both methods can be followed by microscopic observations, small angle light scattering (SALS), or rheo-optics. Because of the applied shear flow, the droplets are deformed and form ellipsoidal droplets. At steady-state deformation, the viscous forces that act on the droplet are balanced by the interfacial forces. Assuming that the interfacial tension is the only parameter that contributes to the interfacial forces, one can determine the interfacial tension from the viscous forces that are applied.[17] However, we will show that in the case of biopolymer mixtures the interfacial tension is not the only parameter that contributes to the deformation and relaxation behavior. Biopolymer mixtures exist of more than 90% water. When these mixtures phase separate, the main ingredient of both coexisting phases is water. These systems can thus be considered as water-in-water emulsions. Since the solvent (water) does not have any preference to stay in either the upper or lower phase, water can diffuse through the interface depending on the forces that act on the system. These interfaces can thus be compared with membranes that have a permeability.[18] This permeability can contribute to the deformation and relaxation behavior and can therefore influence the morphologies of the systems.

Experiments have shown the importance of this permeability. In spinning drop experiments (results reported elsewhere), we observed that the volume of dispersed droplets reduced by approximately 90% in approximately 10 days. This paper will focus on the effect of the permeability on the relaxation of droplets after cessation of shear flow.

Experimental Section

Materials and Methods. To obtain aqueous phase-separated biopolymer mixtures, we have mixed the protein gelatin with the polysaccharide dextran in water. At low concentrations, these mixtures phase separate into two clear phases, with the lower phase enriched in dextran and the upper phase enriched in gelatin. All experiments are performed at room temperature (25 °C). We have used a high molecular weight fish

* Corresponding author. Electronic mail: erik.vanderlinden@wur.nl.

10.1021/bm050721w CCC: $33.50
Published on Web 12/17/2005

gelatin (instead of mammalian gelatin), with a low gelling temperature, to ensure that all mixtures stay liquid at room temperatures. The high molecular weight gelatin was kindly provided by Norland Products Incorporated, Cranbury, U.S. The molecular weight, M_w, of the gelatin is 102 kDa. The dextran was purchased from Sigma-Aldrich and has a molecular weight, M_w, of 511 kDa.

Preparation of the Biopolymer Mixtures. The mixtures of gelatin and dextran were prepared by dissolving these biopolymers simultaneously in a 0.05 M NaI solution. This low molar salt solution was used to enhance the solubility of the gelatin. Sodiumazide (0.02%) was added as an antimicrobial agent. The mixtures were allowed to stand overnight, after which they were heated at 40 °C for about 30 min and shaken frequently to obtain homogeneous mixtures. After they were cooled to room temperature, they were allowed to stand in order for the separation to complete. For the concentrated mixtures, this could take a few days/weeks. A faster method to obtain two separated phases would be to centrifuge at high speeds. However, centrifugation might influence the phase behavior of the system, since the interfaces are thought to be permeable. This could induce a nonequilibrium state of the mixture, and therefore, we chose not to follow this procedure. After the mixtures were completely separated, the upper phase was removed from the lower phase.

Determination of Concentrations of Biopolymers in Both Phases. The concentration of biopolymers in mixtures was determined by measuring the optical rotation with a Perkin-Elmer polarimeter. Before the mixtures were measured, they were diluted 20−50 times. The details of this analysis technique are described elsewhere.[19]

Determination of Viscosity of Both Coexisting Phases. To determine the viscous forces that act on the droplets, the viscosities of both the lower phase and the upper phase were determined. Here, we make use of the intrinsic viscosities of both biopolymers. The viscosity of a polymer solution can be described by[20]

$$\eta_{rel} = 1 + [\eta_0]\cdot c + \frac{1}{25}([\eta_0]\cdot c)^{7/2} \quad (1)$$

in which η_{rel} is the relative viscosity of the solution, η_0 the intrinsic viscosity, and c the concentration of the biopolymer. The intrinsic viscosity is a specific property of a biopolymer. When two different biopolymers are mixed, we assume that the intrinsic viscosity of the mixtures can be described as a function of the separate intrinsic viscosities as

$$[\eta_0]_{mix} = [\eta_0]_1\cdot f_1 + [\eta_0]_2\cdot f_2 \quad (2)$$

where f_i is the mass fraction of polymer i. By inserting this intrinsic viscosity of the mixtures in eq 1 and taking c as the total biopolymer concentration, the relative viscosity of the biopolymer solution can be calculated. The relative viscosity of seven samples of both gelatin and dextran, with concentrations ranging from 1 to 100 mg/mL, were measured with Ubbelohdes at room temperature (25 °C). From these measurements, the intrinsic viscosities of gelatin and dextran were deduced and used to calculate the intrinsic viscosity of mixtures. Equation 2 is valid only when the intrinsic viscosity of a mixture is a simple addition of the separate contributions. To test whether this relation holds for the concentration regime of the experiments, the viscosity of mixtures of gelatin and polysaccharides were measured and compared to the determined viscosity according to eq 2. The calculated values were in good agreement with the experimental values (within 5% deviation).

Relaxation Experiment. To be able to tell whether the permeability contributes to the relaxation of deformed droplets in cessation-of-flow experiments, we have performed relaxation measurements. When droplets are subjected to a shear flow $\dot{\gamma}$, the droplets will deform because of the viscous forces that act on the droplet. After cessation of the flow, the interfacial forces will induce a retraction of the droplet to the energetically more favorable spherical shape. For these experiments, six samples were used with different concentrations of the polysaccharide and a fixed concentration of gelatin. After the separation of the phases, the upper phase was redispersed into the lower phase with a ratio of 0.075 (volume-based). The dispersions were poured into a parallel-plate shear cell (Linkam Scientific Instruments, type CCS 450), with a rotating lower plate and a fixed upper plate. The shear cell is mounted on a microscope (Zeiss Axioskop 2 plus) equipped with a CCD camera (Hitachi CCD color camera). A shear rate was chosen in the range from 0.01 to 0.2 s^{-1}. (The relaxation time of the droplets is assumed to be independent of the shear rate.) The gap size between the plates was adjusted to at least 4 times the droplet size, to exclude possible wall effects. The dispersions were subjected to a shear flow until an equilibrium size was obtained, and then, the shear flow was stopped. The retraction of the droplet after the cessation of flow was recorded with a speed of 5 frames per second. By analyzing the different frames, the deformation of the droplets can be followed in time.

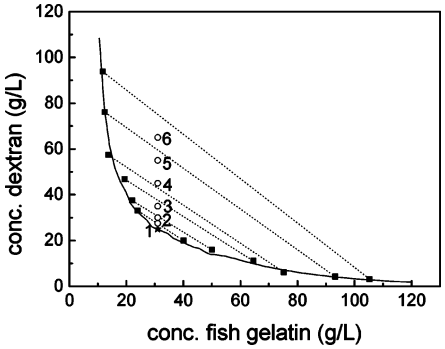

Figure 1. Phase diagram of the gelatin/dextran system. The open circles refer to the overall compositions, the star denotes the critical point, and the squares refer to the compositions of the coexisting phases.

The deformation is determined using the approach as used by, e.g., Mellema et al. [21] A weakly deformed sphere with an initial radius R_0 can be described in spherical coordinates by[22]

$$R(\theta, \phi) = R_0 + s(\theta, \phi) \quad (3)$$

The function $s(\theta, \phi)$ can be expanded in spherical harmonics. Here, we approximate $s(\theta, \phi)$ by the second-order Legendre polynomial $s = (^1/_2)s_2(3\cos^2\theta - 1)$, where s_2 is the amplitude of the deformation, equal to $(^2/_3)(a - b)$. The parameters a and b are the major axis and minor axis of the deformed droplet. The time evolution of the amplitude of deformation can be expressed as

$$s_2 = s_0 \exp\left(\frac{-t}{\tau}\right) \quad (4)$$

in which s_0 is an unknown parameter, t is time, and τ is the characteristic relaxation time for the given system. The deformation of the droplet in time gives the system-specific relaxation parameter τ. Expressions that link this parameter to the viscosity of the phases and interfacial properties are discussed in the next section.

Results and Discussion

Phase Behavior and Distribution of Biopolymers. We have studied six samples with varying composition and varying distance from the critical point. The concentration of gelatin was kept constant, while the concentration of the polysaccharide varied. The samples were allowed to phase separate, after which the phases were separated from each other with a syringe. The optical rotation of both phases was determined with the use of polarimetry, from which the concentrations of both biopolymers in both phases could be determined. The phase diagram is given in Figure 1. The overall concentrations and the distribution in both the upper and lower phases are given in Table 1.

Table 1. Overall Concentrations and Distribution of Both Biopolymers

	overall concentrated fish gelatin[a]	overall concentrated dextran[a]	upper phase		lower phase	
sample	(g/L)	(g/L)	concentrated gelatin	concentrated dextran	concentrated gelatin	concentrated dextran
1	31	30	40	21.5	32.0	27.5
2	31	35	50	16.0	22.0	37.5
3	31	40	64.5	11.1	19.3	46.8
4	31	45	75.2	6.1	13.7	57.4
5	31	55	93.2	4.2	12.4	76.1
6	31	65	105.3	3.1	11.7	93.8

[a] Solvent that was used is a 0.05 M NaI solution.

Table 2. Viscosities of Upper and Lower Phase of Used Samples Given in Table 1

sample	phase	$[\eta_0]_{mix}$ (L/g)	η_{rel}	h (mPa·s)
1	upper	0.059	8.23	7.3
	lower	0.061	7.59	6.8
2	upper	0.058	9.19	8.2
	lower	0.061	8.37	7.4
3	upper	0.057	12.01	10.7
	lower	0.062	10.69	9.5
4	upper	0.056	13.85	12.3
	lower	0.063	13.05	11.6
5	upper	0.056	21.78	19.4
	lower	0.063	23.32	20.8
6	upper	0.056	29.16	26.0
	lower	0.064	39.10	34.8

Phase Behavior and Viscosities of Separated Phases. The intrinsic viscosity, $[\eta_0]$, of gelatin was determined to be 0.0558 L/g, and the intrinsic viscosity of dextran was determined to be 0.0646L/g. With eq 2, the intrinsic viscosities of any mixture with different fraction of proteins and polysaccharides could be calculated. Inserting this intrinsic viscosity into eq 1 gives the relative viscosity of the mixtures. By using the viscosity of the water at 25 °C ($\eta = 0.89$ mPa·s), these relative viscosities can be converted to the viscosities of the phases, as summarized in Table 2.

Relaxation Behavior. To perform the relaxation experiments, a small fraction of the upper phase was redispersed into the lower phase. A shear rate was applied to break up the droplets to a final size between 20 and 70 μm (experimental size limit). Figure 2 shows an example of the retraction of droplets. Only droplets that have no contact with any other droplet were taken into account, to avoid interaction effects between the droplets.

The deformation amplitude, s_2, was determined at different times from the pictures that were taken with the camera. Plotting this deformation factor versus time, and using eq 4, the characteristic relaxation times, τ, for the retraction of different droplets were determined for all six samples. Oldroyd[17] showed that for viscous liquids this characteristic relaxation time is given by

$$\tau = \frac{\eta R_0}{\gamma}\left[\frac{(19E + 16)(2E + 3)}{40(E + 1)}\right] \qquad (5)$$

in which η is the viscosity of the continuous phase, R_0 is the size of the droplet after retraction, γ is the interfacial tension, and E is the viscosity ratio of the dispersed and continuous phases. This expression has been used for polymer blends[2] and biopolymer solutions,[10−12,16] using known values for the viscosities of the phases and measured values of the characteristic relaxation time of a single droplet of size R_0. However, determination of the interfacial tension from just one droplet size is not very accurate, and precision can be improved by measuring the relaxation as a function of R_0. Plotting τ versus R_0 should yield a straight line, from which the interfacial tension can be determined. Figure 3a−f gives an overview of these plots for samples 1−6.

A straight line was fitted through the data points of each sample, and the slope was used to calculate the interfacial tension, using eq 5, and the data from Table 2. The calculated interfacial tensions are given in Table 3.

From these data, we can see that the interfacial tension increases with an increase in dextran concentration. The order of magnitude is comparable to values that have been measured before for gelatin/dextran systems.[19,23] In Figure 3, the lines through the data points show a nonzero intercept on the y-axis. Equation 5 predicts that these lines should go through the origin. This is clearly not the case for any of the systems, and therefore, eq 5 is not an adequate representation of our data. The existence of an intercept indicates that the interfacial tension and the viscosities of the phases are not the only parameters that play a role in the retraction of droplets after cessation of a flow field.

Scholten et al.[24] showed recently that, in systems with ultralow interfacial tension, bending rigidities might become important and could play a role in interfacial phenomena, such as phase separation.[25] This parameter might also play a role in the retraction of droplets and might have to be taken into account in the description of the interfacial forces. From earlier calculations, the bending rigidities were estimated to be a few hundred k_bT for near-critical systems with a very large interfacial thickness.[24] These calculations showed that bending rigidities become important at droplet sizes smaller than a certain critical radius, R_c, which is equal to $\sqrt{2k/\gamma}$. Taking realistic values for k (100 k_bT) and γ (1 μN/m), we find a critical radius of approximately 2 μm. However, for the relaxation measurements, we used droplets with radii between 20 and 80 μm, which is

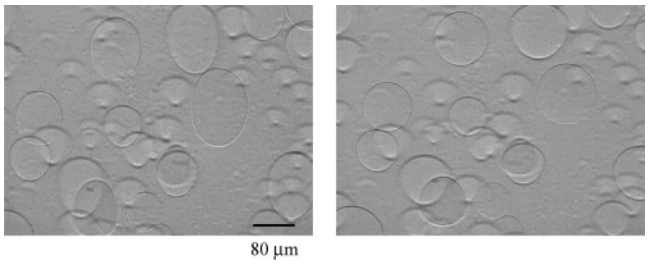

Figure 2. Retraction of droplet after cessation of flow: dispersed droplets of sample 2. The left picture shows the deformation before cessation of the flow field. The right picture shows the droplets at the end of the retraction where they regain their spherical shape. The droplets elongate in the direction of the flow field.

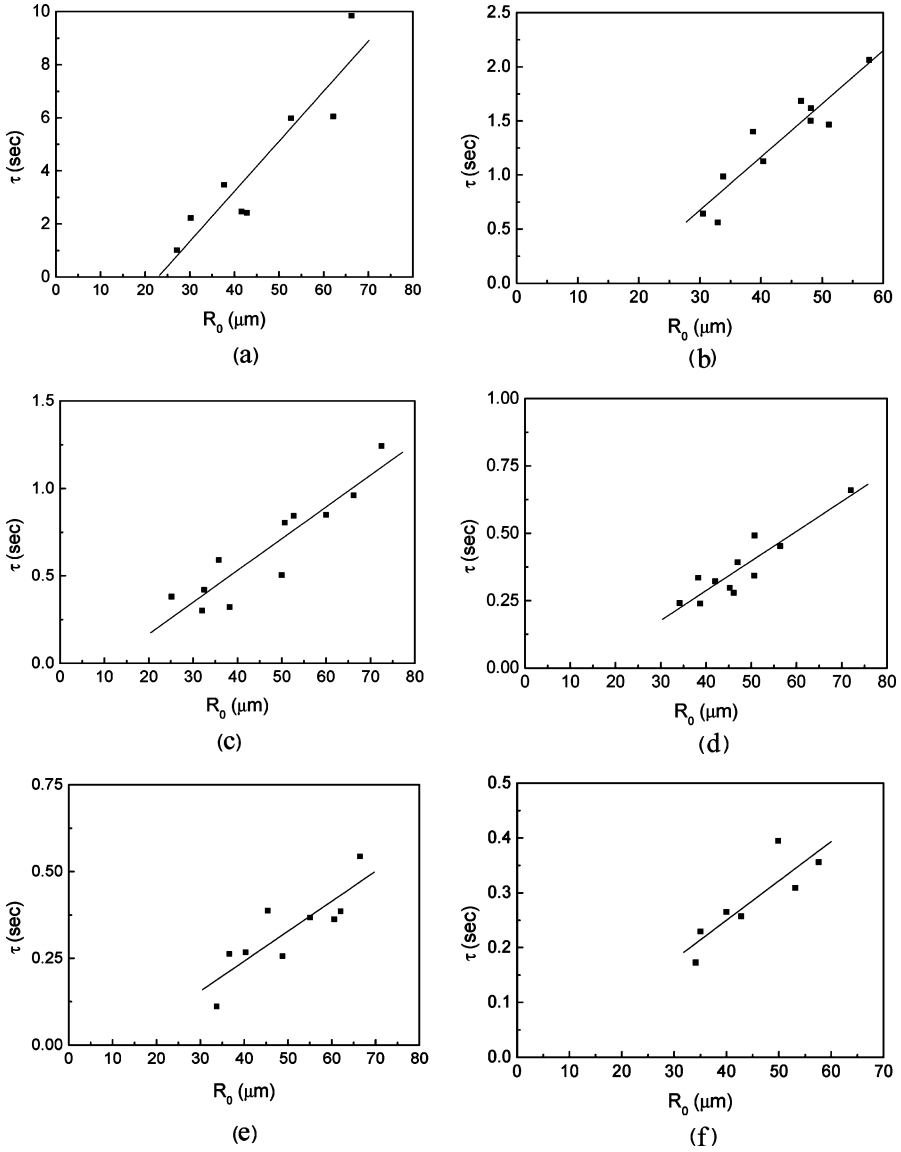

Figure 3. Characteristic relaxation time, τ, plotted vs the radius of deformed droplet, R_0: (a) sample 1, (b) sample 2, (c) sample 3, (d) sample 4, (e) sample 5, and (f) sample 6. For composition of these samples, see Table 1. The line is a linear fit through the data points, from which the interfacial tension is determined.

Table 3. Interfacial Tension for the Gelatin/Dextran Samples Given in Table 1

sample	γ (μN/m)
1	0.15 ± 0.01
2	0.3 ± 0.1
3	1.2 ± 0.2
4	2.4 ± 0.3
5	5.1 ± 0.9
6	9.2 ± 1.9

much larger than the critical radius below which the bending rigidity has to be taken into account. The contribution from the bending rigidity to the interfacial energy should be negligible for the droplet sizes that were used and should not give a large effect in the relaxation time of the retracting droplets. Therefore, the intercept in Figure 3 cannot be attributed to the bending rigidity.

Shi et al.[26] published results on interfacial tension measurements of polydisperse immiscible polymers (PDMS and PIB). They measure the interfacial tension with the pendant drop technique and observe that it decreases with time (minutes to hours). They ascribe this effect to the polydispersity of the polymers. Since the interfacial tension depends on the size of the components at the interface, the smaller components migrate to the interface, thus lowering the energy of the system. Although they show this effect in the pendant drop method only, they expect this migration to occur also in shear experiments, but at time scales much shorter than for the pendant drop technique. Since our biopolymers are polydisperse (dextran has a polydispersity of 1.5 and fish gelatin of 2.7), this effect might occur in our experiments as well. When the migration time is on the same order of magnitude as the relaxation time, this effect might influence the value of the relaxation time, since the diffusion of low molecular weight components would change the interfacial tension during the measurement. This effect would be different for various droplet sizes, since the relaxation time of the droplets is different. However, Shi et al.[26] expect the migration time for shear experiments to be much shorter than the time scale in our experiments, which means that no effect of migration will be observed. Even if the migration time is on the same order of magnitude, the migration effect does not seem to explain our experimental results. From their results, with

polymers that have a similar degree of polydispersity as ours, they see that the interfacial tension decreases up to 15% only, which could never explain the large deviation from the origin in our plots.

The results from Figure 3 show that besides the interfacial tension other interfacial properties may be involved in the relaxation of droplets. One of the parameters that could play a role is the permeability of the interfaces. Other experiments (results reported elsewhere) show that the interfaces in aqueous phase-separated biopolymer mixtures are indeed permeable and that all ingredients can diffuse easily through the interface from one bulk phase into the other. In these experiments, one droplet (approximately 1 μL) of the upper phase was dispersed into a matrix of the lower phase in a capillary of a spinning drop tensiometer. The balance between an applied centrifugal force and the interfacial forces leads to a deformation of the droplet into a more elongated shape. In these experiments, the volume and the shape of the droplets were recorded as a function of time. The results show that the droplets show a decrease in volume of about 90% in days to weeks, which can only be explained if we assume water and both biopolymers to diffuse through the interface. The permeability of the interface may also play a role at shorter time scales.

By taking into account the permeability of the interface, we are including a second mechanism for droplet relaxation. Apart from the retraction driven by interfacial tension forces, we are allowing the deformed droplets to relax by transferring mass across the interface. The volume flux of mass, j (m/s), across the interface is proportional to $\lambda \cdot \Delta P \propto \lambda\gamma/R_0$, where λ is the permeability of the interface and ΔP is the Laplace pressure of the sphere. The volume flux is also proportional to R_0/τ. Hence, by accounting for mass transfer across the interface, we introduce an additional relaxation mechanism with a characteristic time $\tau \propto R_0^2/\lambda\gamma$. If we assume that both relaxation mechanisms act in parallel, then the expression for the overall relaxation time of the system is given by

$$\frac{1}{\tau} = A\frac{\gamma}{\eta R_0} + B\frac{\lambda\gamma}{{R_0}^2} \tag{6}$$

In this equation, A and B are prefactors. This equation resembles a relation suggested by Prost et al.,[18] who studied the fluctuations of membranes as a function of porosity. The values for A and B could be deduced from the exact profiles of the flow inside and around the droplets. We will assume that, since, in the limit of zero permeability, eq 6 should reduce to eq 5, the prefactor A is equal to $[40(E + 1)/(19E + 16)(2E + 3)]$. Prefactor B is unknown, so, for reasons of simplicity, we exchange $B\lambda$ by an effective permeability, λ_{eff}, where we expect B to be on the order of 1 for biopolymer systems (since $E \approx 1$).

Rewriting eq 9 gives the following expression for the relaxation time

$$\tau = \frac{\eta R_0}{\gamma}\left(\frac{1}{A + \dfrac{\lambda_{\text{eff}}\eta}{R_0}}\right) \tag{7}$$

which we have used to fit the experimental data (given as squares in Figure 4) to see whether the permeability plays a role in the relaxation experiments. The best fits through the data points are given as the solid lines. As can be seen, the fitted lines go through the data points as well as the origin, which was not the case when using eq 5. This shows that indeed the permeability of the interface has to be taken into account in a full description of the relaxation of deformed droplets. If this permeability is not taken into account, the interfacial tension will be overestimated, especially when the interfacial tension is deduced from the relaxation time of only *one* droplet size.

Table 4 gives the results for γ and λ_{eff} from the fits through the data points. For sample 1, we were not able to get a good fit. When the interfacial tension is very low and the permeability very high, the second term in eq 6 is dominant. Since both the interfacial tension and the permeability are present in the numerator of this term, it is difficult to fit both λ_{eff} and γ independently. For values larger than $1 \cdot 10^{-8}$ N/m, a satisfactory fit through the data points could not be found. For any value smaller than this, any combination of γ and λ_{eff} gave a good fit. This indicates that the interfacial tension must be smaller than $1 \cdot 10^{-8}$ N/m. Consequently, the value for the permeability should be larger than approximately $5 \cdot 10^{-2}$ m^3/N·s, since below this value a fit through the data points is not in agreement with the experimental data.

The error margins in both the interfacial tension and the permeability are substantial. This can be explained by the fact that the data points from the experiments show a fairly large scatter, which is a result of the method that we use. Since we have only one rotating plate, it is not possible to measure the same droplet several times, so the relaxation time can only be measured once for different droplet sizes. The relaxation process is recorded with a frame grabber with a speed of 5 frames per second. The amount of data points to deduce the specific relaxation time τ is therefore limited to the speed of the frame grabber. The faster the relaxation process, the less accurate is the determination of the relaxation time. These experimental limitations cause the scatter in the data points, which has its influence on the error margins of the interfacial properties. This explains the large error margins in the permeability of samples 5 and 6. The results could be improved by using a shear cell with two rotating plates in opposite direction. This would allow multiple measurement of a single droplet, from which an average could be taken. The use of a faster frame grabber would improve the determination of the relaxation time τ.

To show that the permeability indeed plays a role, we plot $[(1/\tau - A\gamma/\eta R_0)/\lambda_{\text{eff}}\gamma]$ versus $(1/R_0^2)$, using the values from the fit of eq 5 (Table 4). This should give a master curve with a slope equal to 1 when the permeability plays a role in the relaxation process. Figure 5 shows that the data of all samples are located around a line with a slope of 1, which indicates that the permeability indeed has to be included for a full description for the relaxation process.

From Table 4, we see that the interfacial tension for sample 1 is at the most $1 \cdot 10^{-8}$ (N/m), while the value was $1.5 \cdot 10^{-7}$ when calculated without taking the permeability into account. This is a difference of about 90%. With increasing interfacial tension, the difference in the interfacial tension (with or without the contribution of the permeability) decreases. Since the distance from the critical point increases when going from sample 1 to 6 (going further into the two-phase state in the phase diagram), we can conclude that the deviation in the interfacial tension becomes large for samples close to the critical point and diminishes when going further from the critical point. For samples far from the critical point, the interfacial tension as deduced from eq 5 will give satisfactory results. However, when systems are close to the critical point and the interfacial tension is very low, the interfacial tension as determined from eq 5 is overestimated. For these systems, the permeability has to be taken into account for a full description of the relaxation time, and the interfacial tension must be determined using eq 7.

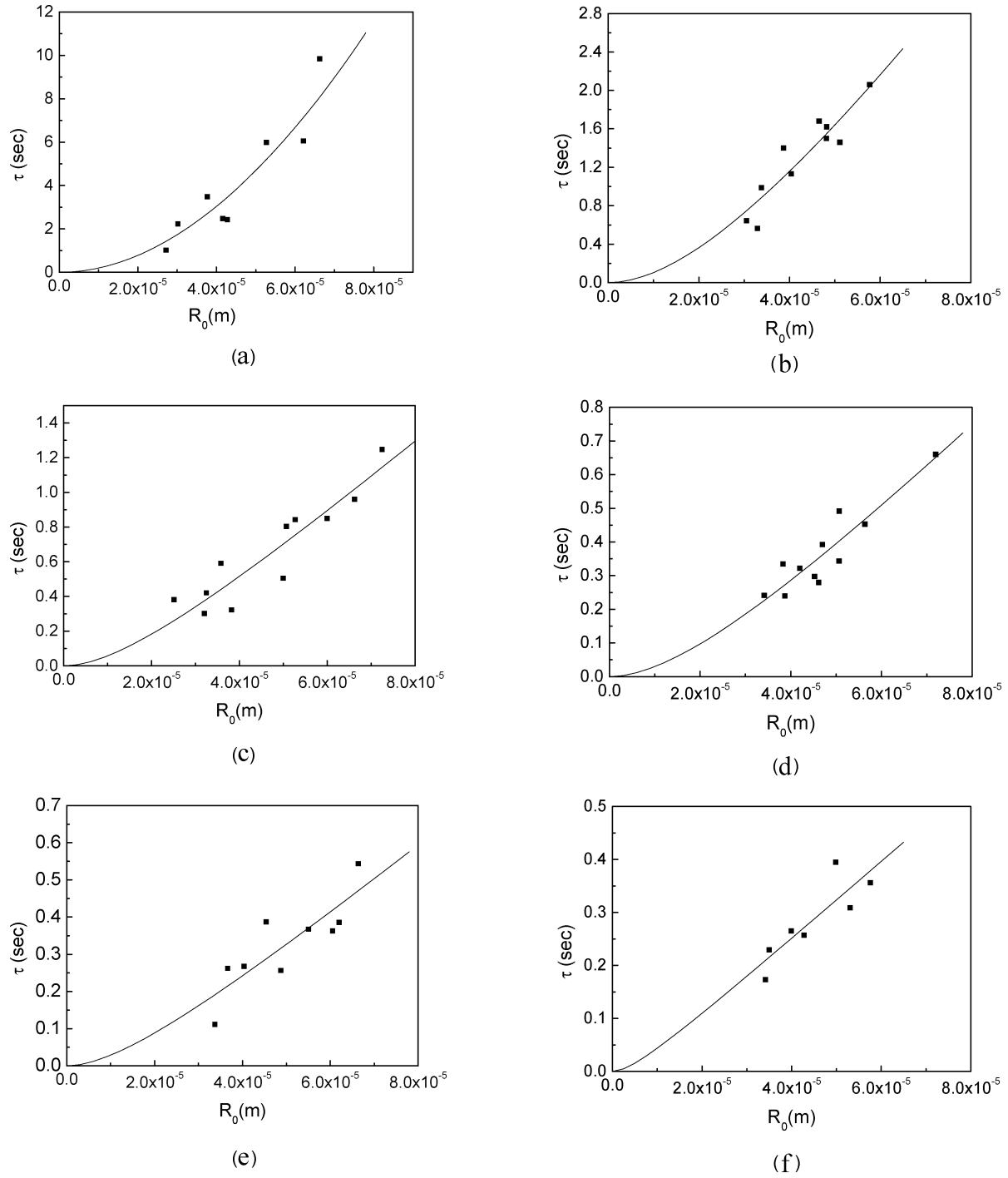

Figure 4. Characteristic relaxation time, τ, plotted vs the radius of deformed droplet, R_0: (a) sample 1, (b) sample 2, (c) sample 3, (d) sample 4, (e) sample 5, (f) sample 6. The line is the best fit to eq 10, from which the interfacial tension and the permeability are calculated.

Table 4. Interfacial Tension (γ) Calculated with Eq 7, the Interfacial Tension (γ) Calculated with Eq 5, and the Permeability, λ_{eff}, of Samples 1−6

sample	γ (μN/m)	γ (μN/m)	λ_{eff} (m^3/N·s)
1	≤0.01	0.15 ± 0.01	$\geq 5 \cdot 10^{-2}$
2	0.2 ± 0.1	0.3 ± 0.1	$3.4 \cdot 10^{-3} \pm 1.1 \cdot 10^{-3}$
3	1.0 ± 0.3	1.2 ± 0.2	$1.3 \cdot 10^{-3} \pm 0.6 \cdot 10^{-3}$
4	1.9 ± 0.6	2.4 ± 0.3	$1.4 \cdot 10^{-3} \pm 0.5 \cdot 10^{-3}$
5	4.6 ± 2.2	5.1 ± 0.9	$5.3 \cdot 10^{-4} \pm 5.2 \cdot 10^{-4}$
6	9.2 ± 3.2	9.2 ± 1.9	$9 \cdot 10^{-5} \pm 2.2 \cdot 10^{-4}$

Table 4 also shows the effective permeability of the interfaces (when prefactor B is known, these values can be converted to exact values for the permeability). Looking at the trend of the permeability of the interfaces, we see that the permeability increases with a decrease in interfacial tension. Thus, for a lower interfacial tension, the permeability plays a more important role, which explains the large difference in interfacial tension for sample 1. The higher the interfacial tension, the less important the permeability is.

From these results, we can see that indeed these interfaces are very permeable to the ingredients in the system. The smaller the interfacial tension is, the higher the permeability is. When the interfacial tension is small (close to the critical point), the composition of both phases is alike, and the water can diffuse easily through the interface. For systems further from the critical point (with larger interfacial tension), the composition of the

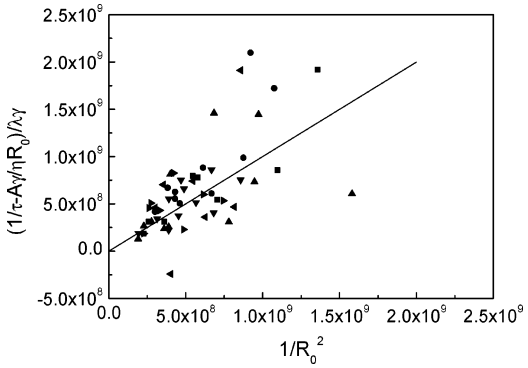

Figure 5. $[1/\tau - (A\gamma/\eta R_0)\lambda_{eff}\gamma]$ plotted as a function of $(1/R_0^2)$ for sample 1 (■), sample 2 (●), sample 3 (▲), sample 4 (▼), sample 5 (triangle right solid), and sample 6 (triangle left solid). The line has a slope equal to 1.

Table 5. γ, λ_{eff}, and Interfacial Thickness, ξ, for Samples 2−6

sample	γ (μN/m)	λ_{eff} (m³/N·s)	ξ (nm)
2	0.2	$3.4\cdot10^{-3}$	340
3	1.0	$1.3\cdot10^{-3}$	215
4	1.9	$1.4\cdot10^{-3}$	220
5	4.6	$5.3\cdot10^{-4}$	105
6	9.2	$1.0\cdot10^{-4}$	53

phases differ more, and this results in a lower permeability (more pressure is needed to push the water through the interface). The interfacial tension, and subsequently the distance from the critical point, can be related to the thickness of the interface as $\gamma \propto 1/\xi^2$.[27,28] Since the permeability decreases with increasing interfacial tension, the permeability should increase with increasing interfacial thickness. To see whether this is true, we have calculated the interfacial thickness according to a method described elsewhere.[24] This method uses the measured interfacial tension and the interaction potential between the biopolymers to calculate the interfacial thickness. Table 5 shows the interfacial tension, the permeability of the system, and the interfacial thickness. We will leave the values for sample 1 out of consideration, since the best values for the fit are not known. From the data, we indeed see that the permeability increases with increasing interfacial thickness.

To investigate the scaling relation between the permeability of the interface with other interfacial properties, we have plotted the permeability versus the interfacial tension and the interfacial thickness. Figure 6 shows the permeability versus the interfacial tension. The data were fitted to the relation $\lambda_{eff} \propto \gamma^a$, for which the exponent $a = -0.9$ gave the best fit. Figure 7 shows the

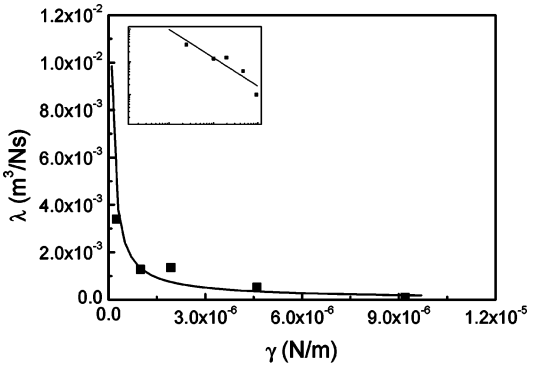

Figure 6. Permeability, λ_{eff}, plotted vs the interfacial tension, γ. The squares refer to the experimental data points. The solid line is the scaling relation $\lambda_{eff} \propto \gamma^{-0.9}$. The inset shows a double logarithmic plot.

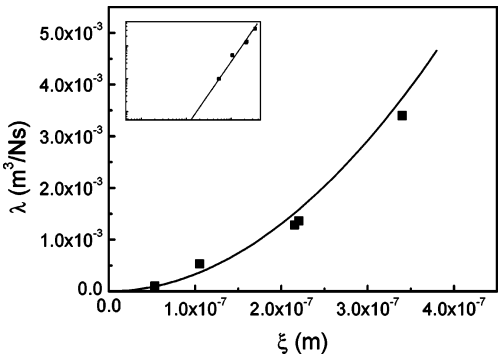

Figure 7. Permeability, λ_{eff}, plotted vs the interfacial thickness, ξ, as given in Table 5. The squares are the experimental data points. The solid line is the scaling relation $\lambda_{eff} \propto \xi^{2.0}$. The inset shows a double logarithmic plot.

permeability versus the interfacial thickness, for which the data was fitted to the relation $\lambda_{eff} \propto \xi^b$. The best fit gave an exponent $b = 2.0$.

Thus, the permeability seems to be inversely related to the interfacial tension $\lambda_{eff} \propto 1/\gamma$ and related to the square of the interfacial thickness, $\lambda_{eff} \propto \xi^2$. This is what we would expect, since the interfacial tension is related to the interfacial thickness as $\gamma \propto 1/\xi^2$.

Since the interfaces of these water-in-water emulsions are permeable, all components could be able to diffuse through the interface in the relaxation process. The self-diffusion coefficient ($D_{self-diffusion} = kT/6\pi\eta R_h$, where R_h is the hydrodynamic radius) of the biopolymers is much smaller than that of water because of the large difference in the hydrodynamic radius. Taking into account the short time scale of the experiments, we assume that only the water diffuses through the interface in these relaxation experiments. For ordinary diffusion over a distance R_0, the scaling relation for the relaxation time is given by

$$\tau \approx \frac{R_0^2}{D} \tag{8}$$

where D is the diffusion coefficient. Comparing eq 8 with the second term of eq 6, we see that the product of the interfacial tension and the permeability represents an effective diffusion coefficient, $D_{eff} \propto \lambda_{eff}\cdot\gamma$. Rewriting this expression leads the to following relation for the permeability of the interface, $\lambda_{eff} \propto D_{eff}/\gamma$. Since the permeability is inversely proportional to the interfacial tension ($\lambda_{eff} \propto 1/\gamma$), the diffusion coefficient should be constant. Thus, the diffusion coefficient is independent of the concentration of the ingredients that are present in the concentration regime of these systems. Since the water molecules are much smaller (Å) than the mesh size of the biopolymer solutions, which are normally on the order of nanometers, the water molecules are probably not slowed by the polymer network, but diffuse through the network with ease. Using the relation for the interfacial tension and the interfacial thickness, $\gamma \propto 1/\xi^2$, we see that the permeability is also proportional to $\lambda_{eff} \propto D_{eff}\xi^2$. From this relation, we see that the permeability is independent only of the diffusion coefficients of the water molecules and the thickness of the interface.

Using $\lambda_{eff} \propto D_{eff}/\gamma$, we can determine the diffusion coefficient from the plot of λ_{eff} versus $1/\gamma$, which is given as Figure 8. The slope of the fit through the data points is equal to $0.9\cdot10^{-9}$ m²/s. This is comparable to values found by Yapel et al.,[29] who measured the self-diffusion of water through gelatin gels with different water content by pulse-gradient NMR spectroscopy. They found values ranging from $1\cdot10^{-10}$ to $2.5\cdot10^{-9}$ depending

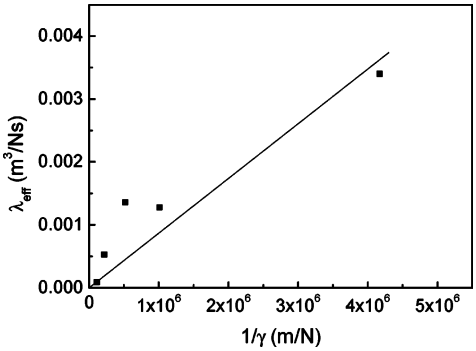

Figure 8. λ_{eff} vs $1/\gamma$. The line is the linear fit through the points, with the origin as a theoretical point.

on the concentration of the gelatin present in the systems. It is also close to the self-diffusion coefficient of water, D_w^0, which is equal to $2.3 \cdot 10^{-9}$ m^2/s. This indicates that indeed only the water diffuses through the interface.

Conclusion

We have performed relaxation experiments on deformed droplets of phase-separated biopolymer mixtures. Our experiments indicate that the permeability of the interface plays an important role in the relaxation of deformed droplets after cessation of flow. These phase-separated mixtures can be regarded as water-in-water emulsions with two coexisting phases that mainly consist of water (for about 90%). The water does not have more affinity to be in either one of the phases, and therefore, the water can diffuse through the interface. From our experiments, we see that, without taking this permeability into account, the interfacial tension is overestimated for samples very close to the critical point, with very low interfacial tensions. For these samples, where the phases are almost alike and the interfacial thickness is very large, the permeability is very high. The permeability decreases for increasing interfacial tension (going further from the critical point). From scaling relations, we found that the permeability is inversely proportional to the interfacial tension ($\lambda_{eff} \propto 1/\gamma$) and related to the square of the interfacial thickness ($\lambda_{eff} \propto \xi^2$). The effective diffusion coefficient was determined from $\lambda_{eff} \propto D_{eff}/\gamma$ and was found to be close to the value of the self-diffusion coefficient of water. This indicates that only the water diffuses through the interface. From the results, we see that the diffusion coefficient is independent of the composition of the mixtures and the concentration regime that is used. Since the size of the water molecules is much smaller than the mesh size of the polymer networks, the water molecules are assumed to diffuse through the networks without any hindrance of the biopolymers.

Acknowledgment. We thank J. Prost (Institut Curie, Paris, France) for helpful discussions.

References and Notes

(1) Son, Y.; Yoon, J. T. *Polymer* **2001**, *42*, 7209−7213.
(2) Son, Y.; Migler, K. *Polymer* **2002**, *43*, 3001−3006.
(3) Guido, S.; Simeone, M.; Villone, M. *Rheol. Acta* **1999**, *38*, 287−296.
(4) Cavallo, R.; Guido, S.; Simeone, M. *Rheol. Acta* **2003**, *42*, 1−9.
(5) Guido, S.; Villone, M. *J. Rheol.***1998**, *42*, 395−415.
(6) van Puyvelde, P.; Moldenaers, P.; Mewis, J. *Phys. Chem. Chem. Phys.* **1999**, *1*, 2505−2511.
(7) Tassiere, M.; Grizzuti, N.; Greco, F. *Macromol. Symp.* **2003**, *198*, 53−67.
(8) Vermant, J.; van Puyvelde, P.; Moldenaers, P.; Mewis, J. *Langmuir* **1998**, *14*, 1612−1617.
(9) Ziegler, V. E.; Wolf, B. A. *Langmuir* **2004**, *20*, 5826−5833.
(10) Pacek, A. W.; Ding, P.; Nienow, A. W. *Chem. Eng. Sci.* **2001**, *56*, 3247−3255.
(11) Simeone, M.; Alfani, A.; Guido, S. *Food Hydrocolloids* **2004**, *18*, 463−470.
(12) Ding, P.; Wolf, B.; Frith, W. J.; Clark, A. H.; Norton, I. T.; Pacek, A. W. *J. Colloid Interface Sci.* **2002**, *253*, 367−376.
(13) van Puyvelde, P.; Antonov, Y. A.; Moldenaers, P. *Food Hydrocolloids* **2003**, *17*, 327−332.
(14) van Puyvelde, P.; Antonov, Y. A.; Moldenaers, P. *Korea-Aust. Rheol. J.* **2002**, *14*, 115−119.
(15) Lundell, C.; Walkenström, P.; Lorén, N.; Hermansson, A.-M. *Food Hydrocolloids* **2004**, *18*, 805−815.
(16) Guido, S.; Simeone, M.; Alfani, A. *Carbohydr. Polym.* **2002**, *48*, 143−152.
(17) Oldroyd, J. G. *Proc. R. Soc. London* **1953**, *218*, 122−132.
(18) Prost, J.; Manneville, J.-B.; Bruinsma, R. *Eur. Phys. J. B* **1998**, *1*, 465−480.
(19) Scholten, E.; Visser, J. E.; Sagis, L. M. C.; van der Linden, E. *Langmuir* **2004**, *20*, 2292−2297.
(20) Tuinier, R. An exocellular polysaccharide and its interactions with proteins. Ph.D. Thesis, Wageningen University, Wageningen, 1999.
(21) Mellema, J.; Blom, C.; Beekwilder, J. *Rheol. Acta* **1987**, *26*, 418−427.
(22) Winterhalter, M.; Helfrich, W. *J. Colloid Interface Sci.* **1987**, *122*, 583−586.
(23) Antonov, Y. A.; van Puyvelde, P.; Moldenaers, P. *Int. J. Biol. Macromol.* **2004**, *34*, 29−35.
(24) Scholten, E.; Sagis, L. M. C.; van der Linden, E. *J. Phys. Chem. B* **2004**, *108*, 12164−12169.
(25) Scholten, E.; Sagis, L. M. C.; van der Linden, E. *Macromolecules* **2005**, *38*, 3515−3518.
(26) Shi, T.; Ziegler, V. E.; Welge, I. C.; An, L.; Wolf, B. A. *Macromolecules* **2004**, *37*, 1591−1599.
(27) de Gennes, P. G. *Scaling concepts in polymer physics*; Cornell University Press: New York, 1979.
(28) Rowlinson, J. S.; Widom, B. *Molecular theory of capillarity*; Clarendon Press: Oxford, 1984.
(29) Yapel, R. A.; Duda, J. L.; Lin, X.; van Meervall, E. D. *Polymer* **1994**, *35*, 2411−2416.

BM050721W